

Characterisation of recharge mechanisms in a Precambrian basement aquifer in semi-arid south-west Niger

Maman Sani Abdou Babaye^{1,2}, Philippe Orban³, Boureima Ousmane¹, Guillaume Favreau^{4,5},
Serge Brouyère³, Alain Dassargues³

1. Université Abdou Moumouni, Faculté des Sciences et Techniques, Département de Géologie,
BP:10662 Niamey (Niger).

2. Université Dan DickoDankoulodo de Maradi, Faculté des Sciences et Techniques, UMR
SERMUG, Département de Géologie, BP: 465, Maradi (Niger)

3. Université de Liège, Faculté des Sciences Appliquées, DépartementArGEnCo, Laboratoire
d'Hydrogéologie et Géologie de l'Environnement,

4. IRD, UMR HydroSciences, Université de Montpellier, 163, rue Auguste Broussonet, 34090
Montpellier, France

5. Univ. Grenoble Alpes, Institut de Recherche pour le Développement (IRD), CNRS, Institute
of Engineering Univ. Grenoble Alpes (G-INP), Institut des Géosciences de l'Environnement
(IGE), F-38000 Grenoble, France.

Corresponding author: babaye.sani@gmail.com

Abstract

In the central part of the semi-arid Dargol Basin of southwestern Niger, most of the groundwater resource is contained in the fractured aquifers of the Precambrian basement. The groundwater resource is poorly characterized and this study is the first attempt to better describe the recharge mechanisms and hydrogeochemical behaviour of the aquifers. Hydrogeochemical and

piezometric methods were combined to determine changes in recharge rate and origin of groundwaters for the shallow weathered aquifer and the deep fissured/fractured aquifer. At the basin scale, the groundwater fluxes towards the Niger River are influenced mainly by topography, with no visual long-term trend in groundwater levels (1980-2009). The hydro-geochemical signature is dominated by the calcic-bicarbonate to magnesian (70%) type. It shows evolution from an open environment with CO₂ and low mineralized water (granitoids, alterites) towards a more confined environment with more mineralized waters (schists). Stable water isotopes ($\delta^{18}\text{O}$, $\delta^2\text{H}$) analysis suggests two main groundwater recharge mechanisms: (i) direct recharge with nearly no post-rainfall fractionation signature and (ii) indirect recharge from evaporated surface waters and/or stream-channel beds. Groundwater tritium content indicates that recharge is mostly recent, with an age less than 50 years ($^3\text{H} > 3 \text{ TU}$), with only 10% indicating low or even no recharge for the past decades. A median value of the groundwater renewal rate estimated from individual values of tritium is equivalent to 1.3% y^{-1} , close to the one determined for groundwater samples dating to the early 1980s, thus indicating no measurable long-term change.

Keywords: Niger, fractured aquifers, hydrochemistry, environmental isotopes, groundwater recharge.

NOTE TO COPYEDITOR – PLEASE INSERT THE FOLLOWING AS A FIRST-PAGE FOOTNOTE:

This article is part of the topical collection “...”

1. Introduction

Since the 1970s, the Sahelian regions of West Africa have experienced climatic variability marked by recurrent droughts (Nicholson 2001, L'Hôte *et al.*, 2002; Sagna *et al.*, 2015). These drought periods are remarkable for their duration at the global scale, and characterized by a reduction of about 20% in precipitation (Taylor *et al.*, 2002; Panthou *et al.*, 2014). In the central Sahel, this has led to a degradation of soil surface conditions and lasting changes in the water balance (Leduc *et al.*, 2001; Séguis *et al.*, 2004; Mahé, 2009). The high population growth (of about 2-3% yr⁻¹) and the estimated extension of cultivated areas (5% in 1960 to 14% in 1990) has been associated to a 28% loss of forest cover (Taylor *et al.*, 2002) and have thus accentuated the effect of land clearance on soil crusting (Favreau *et al.*, 2009). Hydrological studies have also shown the sustained indirect impact of these anthropogenic pressures on surface waters. For example, their effects are reflected in the increase in river flows despite the recurrence of droughts (Mahé *et al.*, 2003). As a consequence of intense and persistent climate and environmental disturbances, it is necessary to consider how these changes affect groundwater (Lapworth *et al.*, 2013, Ibrahim *et al.*, 2014). In Niger, the impact of these changes has been assessed in unconfined sedimentary aquifers (Leduc *et al.*, 2001, Leblanc *et al.*, 2008). Higher piezometric levels observed since the mid-1960s are interpreted as the response to anthropogenic degradations of the vegetation cover, despite the decrease of rainfall (Favreau *et al.*, 2009, 2012).

In the crystalline basement zone, the long-term dynamics of groundwater resources remain unknown. Filippi *et al.* (1990) showed that in the neighboring crystalline basement region of Burkina Faso, plurimetric groundwater level fluctuations are caused by the seasonality of rainfall. For a large Sahelian catchment (20,000 km²) in Burkina-Faso, a clear link has been

established (Mahé, 2009) between the degradation of soil surface characteristics and an increase in Hortonian surface water flows. In the basement area of northeastern Mali, Gardelle *et al.* (2010) observed an increase in pond areas which could have an impact on the dynamics of underlying aquifers, if focused recharge occurs similarly to observations made in the sedimentary context of the neighboring Sahelian zones.

Previous research highlights the complexity of hydrogeological studies in semi-arid zones where the different terms of the hydrological balance are particularly sensitive to small environmental changes and where the response of the impacted systems can be counter-intuitive. Despite these difficulties, hydrogeological studies in crystalline basement zones are of primary importance. The uncertainty on water availability is generally more pronounced, since groundwater resources are often smaller in volume and discontinuous in space. In the south-west of Niger, about 40% of the wells drilled in villages have low yield ($<0.5\text{m}^3/\text{h}$). Moreover, 55% of the productive wells are abandoned due to chemical problems, as contaminant concentrations (e.g. nitrate, arsenic, and fluoride) exceed WHO drinking-water standards (Ousmane *et al.*, 2012). These difficulties of access to drinking water, coupled with the low mean productivity, explain why the region's population is locally affected by severe water shortages during the long dry season. In the semi-arid crystalline basement regions, the main challenge lies in a better hydrogeological characterization in order to better understand the groundwater dynamics, not only in terms of recharge, but also in terms of groundwater quality.

Previous studies carried out in the crystalline area of south-west Niger revealed that recharge occurs following two mechanisms: (i) direct and diffuse recharge in some more permeable zones of the landscape (e.g. sand dunes) and, (ii) indirect and punctual recharge in topographical depressions (Ousmane, 1988; Girard *et al.*, 1997; Abdou Babaye, 2012) where water accumulates during the rainy season. Due to the spatial and temporal variability and the various

processes associated with the recharge, estimating the rate of renewal of groundwater is usually challenging in semi-arid areas (De Vries and Simmers, 2002). This complexity is accentuated by the fact that indirect localized recharge is often the dominant recharge mechanism, sometimes at low frequencies (Gaultier, 2004; Bajjali, 2008). Quantification of the localized recharge requires accurate and localized information, which, often over the long term, is unavailable. To compensate for the low density of observations, a range of techniques is commonly used to explain the link between the dynamics of the aquifers and climate and environmental changes (Ngounou Ngatcha *et al.*, 2007, Stadler *et al.*, 2010, Bouragba *et al.*, 2011). In arid and semi-arid regions, multiple tracer approaches are preferred to estimate localized recharge, compared to the regional hydrological water budget method for which accurate quantification of this type of recharge remains difficult (De Vries and Simmers, 2002, Scanlon *et al.*, 2006). In complex water-rock-interaction media, isotopes of the water molecule (^{18}O , ^2H , ^3H) have proven to be valuable tracers of the subsurface flow (among others: Aggarwal *et al.*, 2005; Clark 2015; Solder *et al.*, 2016; Cook *et al.*, 2017).

This study applies hydrodynamics data (groundwater levels, surface water levels) and hydrogeochemical data (major ions, water isotopes) that will be combined to specify, over the long term, the spatio-temporal dynamics of groundwater fluxes in the semi-arid southwest of Niger. This will achieve better management of the resource.

2. Case study

2.1 Geographic and climatic context

The study area is located in the south-western part of Niger, between longitudes $0^{\circ}30'$ and $0^{\circ}50'$ East and latitudes $13^{\circ}45'$ and $14^{\circ}20'$ North. With an area of 900 km^2 , the study area occupies the central part of the Dargol basin, which is a tributary on the right bank of the Niger River (Figure 1). The climate is Sahelian with a rainy season extending from June through September.

The extreme daily temperature values observed over the period 1999-2008 range from 15° C (6 am) to 43° C (6 pm), with an annual average of 29° C. The relative humidity of the air shows an annual variation of 18% (March) to 90% (August). The mean annual rainfall at the Tera rainfall station is 409 mm (1999-2008), while the mean annual evapotranspiration calculated from the Penman method for the corresponding period is 2,000 mm (i.e. five times the annual rainfall). 25% of precipitation is from high-intensity events (Panthou *et al.*, 2014) that produce rapid Hortonian flows (Amani and Nguetora, 2002).

The density and orientation of the drainage network is influenced by the topography, the lithology and the tectonic structure of the substratum. Taking its source in Burkina Faso, about 320 m above sea level (m asl), the temporary river Dargol and its main tributary the Tilim flow on the right bank of the Niger river (elevation 198 m asl at the station of Kakassi), about 90 km northwest of Niamey (Figure 1). Its flow is linked to rainfall that begins in June and July and ends three months later with an average flow of $160 \times 10^6 \text{ m}^3/\text{year}$ (1964-1994). There is also a chain of temporary pools or artificial water reservoirs, of which only the Téra dam contains water continuously (available water volume of $7.7 \times 10^6 \text{ m}^3$ at its creation in 1981).

The relief of the area is relatively flat with isolated hills and fixed sand dunes inherited from more arid periods of the Quaternary. These morphological assemblages are notched by usually dry valleys (koris) which drain water towards depressions (valleys, ponds) during the rainy season. Degraded and sparse vegetation (savanna and steppe) occupies the plateaux, whereas the bottom of the valleys and depressions give way to denser woody vegetation. The rate of local population growth was about 3.9% per year over the period 2001 to 2012, with more than 95% of the population living in rainfed agriculture or extensive livestock farming (INS, 2012).

2.2 Geological and hydrogeological context

The bedrock of the study area is formed by a Precambrian basement composed of rocks of the metamorphic belt (green rocks including pyroxenites, amphibolites, epidotites, chloritoschists,

148 metabasalts, metagabbros, greywacke rocks, tuffs, rhyolitic breccias, micaschists, clayey
149 schists, quartzitischists). These rocks show a NNE-SSW orientation. They are separated by
150 Eburnean granitoid bodies (granites, granodiorites and diorites) (Machens, 1973, Soumaila and
151 Konaté, 2005) (Figure 1). In some locations, these massifs contain Archean relics (pegmatites,
152 leptynites) (Machens, 1973, Dupuis *et al.*, 1991). Shallow formations made of alterite (5 to 50
153 m thick), alluvium and colluvium overlie bedrock formations. At the regional scale, four main
154 fracture orientations constitute the major structural features (Abdou *et al.*, 1998, Affaton *et al.*,
155 2000, Abdou Babaye, 2012): N20 ° to N50 °; N60 ° to N90 °; N120 ° to N140 ° and N350 ° to
156 N15 °.

157 In crystalline and metamorphic schists environments, aquifers are developed in the shallow
158 weathered levels (alterites and alluvial deposits) and in the fractures/cracks of the deep
159 basement. These two superimposed aquifers can be considered as connected in some areas
160 (Dewandel *et al.*, 2006). The weathered aquifer is formed by semi-permeable materials with
161 high storage capacity. It covers the upper part of the deep aquifer corresponding to the highly
162 fractured zone due to decompression of the bed-rock with high permeability. The lower part of
163 the deep aquifer corresponds to the compact bed-rock only affected by fractures of tectonic
164 origin (faults). This deep fractured aquifer is generally confined, whereas, in some locations, it
165 is able to drain the upper horizons. Most fractures therefore contribute to aquifer transmissivity
166 but are considered to have a low storage capacity.

167 In the study area, the depth to the water table varies according to the topography, the type of
168 aquifer and season. The shallow weathered layers are located in the valleys (alluvium) and the
169 plateaux (alterites). The depths to the water table, as observed in traditional wells dug in alluvial
170 formations, vary from 1 to 10 m. In modern wells, drilled in alterites, the water depth ranges
171 between 15 and 30 m. Upper parts of the aquifer are very reactive to rainfall fluctuations
172 (Ousmane, 1988) and can dry up during the dry season leading to recurring problems of water

shortage. Deep aquifer parts are, in principle, more promising in terms of productivity and sustainability because of the role played by fractures in the drainage, storage and circulation of groundwater. As a result, these deep aquifers have been the subject of several village water drilling programs to cover the water needs of the population in the crystalline area. Analysis of the data from 140 boreholes (Figure 1) from these programs (1980-2009) allowed for synthesis of the hydrogeological parameters of the study area. The depths of these boreholes vary from 36 to 120 m with an average of 60 m and a standard deviation of 20 m. The best water production flows are generally obtained between 30 and 65 m; 76% of the water is produced in the first 50 m constituting the upper part of the bedrock (Abdou Babaye, 2012). Beyond this depth, transmissive zones are rare. In granitic rocks, the depth limit to these transmissive zones rarely exceeds 50 m, whereas it can reach 60 m (and even slightly deeper) in green rocks (schists) due to the nature and thickness of their weathering products. Lithological diversity and the various tectonic phases influence the hydrogeological properties of basement aquifers and, of course, their productivity. Analysis of the drilling data reveals that water yields are generally low, ranging from 0.5 m³/h to 5 m³/h, with the majority of boreholes being limited to values below 2.5 m³/h. In green rocks, higher water yield (mean of 2.7 m³/h versus 1.9 m³/h in granitoids) are observed. Flow rates greater than 10 m³/h were obtained in boreholes drilled in fractured networks of shear zones.

Hydraulic conductivity values estimated by short-time (4 h) pumping tests range from 2.4×10^{-7} m/s to 3×10^{-5} m/s with averages of 3×10^{-6} m/s and 1.1×10^{-5} m/s respectively observed on granitoids and green rocks. Ousmane (1988) showed statistically that green rocks are more productive with a drilling success rate (flow rate > 0.5 m³/h) of 87% compared to about 60% for granitoid rocks.

3. Methodology

3.1 Groundwater level surveys

In the study area, measurements of static groundwater levels date from the drilling operations. Unfortunately, there is no regular and official monitoring of groundwater levels in rural and even urban waterworks. The absence of a piezometric network and the low density of measurement points did not allow drawing a reliable piezometric map. However, measurements (with a centimeter accuracy) of groundwater levels have been carried out in various topographic (basin, slope, plateau) and geological (schists, granites, weathered rocks) contexts in both high and low groundwater-level periods. Groundwater levels were measured, at the beginning of the day before the pumping activities, at 30 points in May 2009 and 40 points in October–November 2009 and in April–May 2010. In addition to these seasonal campaigns, monthly surveys were made from October 2009 through January 2012. Almost all the measurements were undertaken in wells screened in the bed-rock fractured aquifer. Only six measurements were made in wells drilled in the superficial layers (alterites and alluvium). All the wells being in operation, the measurements were made very early in the morning (between 5 and 8 am) in order to obtain a measurement in conditions close to the static level. This recent dataset has been completed by about 20 older measurements from the early 1980s to evaluate the long-term dynamics of the groundwater levels.

3.2 Groundwater sampling

Forty-five water samples, taken for classical chemical analyses, were taken from shallow wells, boreholes and surface waters. These samples were taken during periods of high (October–December 2009) and low (April–May 2010) groundwater levels. The sampling points were chosen to be representative of the main different geological contexts of the fractured aquifers in the study area. Nevertheless, for the purpose of comparison, three analyses concerned the shallow aquifer and a surface water sample was also collected at the Tera dam.

In addition, most of the points sampled during the period of high groundwater level were also sampled for isotopes analyses. Thus, 22 waterworks (20 boreholes and 2 wells) were sampled for oxygen-18 / deuterium analyses, and 17 sampled for tritium analyses. 5 of these points are corresponding to those already sampled in the 1980s (Ousmane, 1988). In addition, a surface water sample (Tera dam) was taken and analyzed for its water isotope content.

During each sampling survey, physico-chemical parameters (pH, temperature, electrical conductivity) were measured *in situ*.

Measurements and sampling were carried out after at least 30 minutes of pumping in order to obtain groundwater samples more representative of groundwater in the aquifer.

3.3 Chemical and isotope analyses

Chemical analyses (carried out in the HGE-ULg laboratory) have ionic balance errors varying around $\pm 3\%$. Analyses (Ca^{2+} , Mg^{2+} , Na^+ , K^+ , Cl^- , NO_3^- , SO_4^{2-}) were carried out using a Capillary Ion Analysis (C.I.A.) technique. Silica was determined by a Flame Atomic Absorption technique while carbonate (CO_3^{2-}) and bicarbonate (HCO_3^-) ions were calculated after determination of pH and the complete alkalimetric title.

Analyses of the oxygen-18 / deuterium pair were carried out by the IDES Laboratory of the University of Paris-Sud (Orsay, France) and those related to tritium in the HYDROISOTOP laboratory in Schweitenkirchen, Germany. The results of the analyses are expressed in $\delta \text{‰}$ vs V-SMOW. The analytical errors are respectively $\pm 0.2 \text{‰}$ and $\pm 2 \text{‰}$ for oxygen-18 and deuterium. For tritium (expressed as a tritium unit (TU)), the accuracy is $\pm 0.5 \text{ TU}$ with a detection limit of 0.9 TU.

Rainfall data were obtained from the International Atomic Energy Agency (IAEA) network (GNIP, 2011), from Niamey/ORSTOM stations (1992 to 1999) and IRI/Abdou Moumouni University of Niamey in Niger, located at an almost identical (190 m vs 225 m asl) altitude (Ousmane, 1988; Girard, 1993, Taupin *et al.*, 2002, Guéro, 2003, Tremoy *et al.*, 2012).

247

248 **4. Results**

249 **4.1 Hydrodynamics**

250 The monthly monitoring of the static groundwater piezometric levels shows seasonal
251 fluctuations subsequent to the beginning of the rainy season for all ($n = 3$) of the wells surveyed,
252 both in the shallow part of the aquifer in the alterites (shallow wells) and in the deep fractured
253 aquifer (boreholes). The water table decreases from the end of October to early November,
254 reaching the lower levels in May (Figure 2). From the first weeks of July, a rapid (alterites) or
255 progressive (deep fractured aquifer) rise of groundwater levels is observed. Maxima are reached
256 in August - September or even in October, two to four months after the start of the rainy season.
257 The amplitude of fluctuations of groundwater levels between periods of high and low
258 groundwater levels varies from 0.29 m to 13.1 m. The highest amplitudes are observed in the
259 upper areas (plateau, sand dune).

260 Due to the low amount of data, it is not possible to draw a map with hydraulic head contours.
261 However, main flow directions can be derived from the available data (Figure 3). The map of
262 the main groundwater flow directions in the deep aquifer (Figure 3), drawn for the high
263 groundwater level periods (October-November 2009), shows a strong influence of the
264 topography. The directions of the groundwater flows are thus quite similar to that of surface
265 waters, and influenced by the directions of the major fractures, North-East, South-East and
266 West-East. Some small piezometric domes are observed in the west, south-west, north and
267 center corresponding probably to preferential infiltration from pools and artificial reservoirs
268 (dam). The lowest groundwater levels are observed in the southeastern part of the basin in the
269 vicinity of the Tilim plain and its confluence with the flood plain of the Dargol River.

Comparison of the groundwater levels from the 1980s to 2009 shows a decrease in about 65% of the boreholes (13 out of 20 boreholes) (Figure 4); On the other hand, a significant increase is observed in some boreholes, with no clear spatial pattern observed.

4.2 Hydrochemistry

The results of the chemical analyses (synthesis in Table 1; full analyses in Table S1 of the electronic supplementary material (ESM)) reveal that the groundwater is slightly acidic to neutral and characterized by a variable mineralization (ranging from 266 to 1,184 $\mu\text{S}/\text{cm}$). Dam water, sampled in high water conditions (18 December 2009) shows a low mineralization (143 $\mu\text{S}/\text{cm}$). The temperature of the water varies from 29 to 34 °C in all the groundwater samples. The highest values could be overestimated due to surface measurements in periods of high atmospheric temperatures.

281
282
283
284

Table1: Synthesis of the results of chemical and isotopic analyses for the high groundwater level period (The complete data are provided in Table S1 of the ESM)

Chemical elements (mg/L), electrical conductivity (Cond) in $\mu\text{S/cm}$, deuterium excess (d), $\delta^{18}\text{O}$ and $\delta^2\text{H}$ (‰ V-SMOW), TU Tritium Unit

Sample type (n)		Cond 25°	pH	Ca ²⁺	Mg ²⁺	Na ⁺	K ⁺	Cl ⁻	SO ₄ ²⁻	NO ₃ ⁻	CO ₃ ²⁻	HCO ₃ ⁻	$\delta^{18}\text{O}$	$\delta^2\text{H}$	d	³ H (TU)
Green rocks (12)	Min	385	6.43	18.72	10.51	19.71	2.12	2.67	3.69	0.3	0.93	146.81	-2.32	-11.6	4.78	<0.9
	Max	1,123.3	7.3	128.28	48.66	76.97	7.2	23.43	294.95	231.1	10.54	390.18	-4.49	-31.1	8.24	4.7
	Mean	658.47	6.86	54.7	26.06	47.1	4.32	9.26	57.27	51.25	4.91	278.71	-3.55	-21.9	6.52	3.51
	Stand. Dev	255.60	0.24	33.81	12.37	19.92	1.86	7.211	88.56	69.29	2.37	64.345	0.87	6.96	1.36	1.41
Granitoids (13)	Min	350	6.1	21.8	5.51	13.06	0.01	3.5	2.22	1.05	0.94	100.41	-4.13	-0.09	-0.39	1.4
	Max	1,184.5	7.1	108.1	26.86	84.06	5.17	45.22	40.67	405.8	7.41	353.6	0.9	-27.6	9.56	5.9
	Mean	594.65	6.63	51.57	17.69	49.51	2.93	16.77	19.59	95.84	3.36	228.73	-2.94	-19.2	4.38	3.75
	Stand. Dev	298.98	0.27	26.02	15.39	21.90	1.517	13.3	12.25	124.6	1.93	80.43	1.52	8.24	4.64	1.21
Alterites (1)	-	719	7.1	74.78	27.38	33.62	6.26	42.10	21.75	138.24	3.95	211.25	0.19	-3.06	-4.58	-
Dam (1)	-	143.6	7.79	21.34	3.09	3.51	3.60	1.34	1.29	3.04	0.31	89.56	0.79	-1.99	-1.2	-

285
286

The deep and shallow aquifers show diversified facies (Figure 5). The most represented groundwater facies is the calcium-magnesium bicarbonate facies (70% of the samples) followed by the calcium chloro-sulfate (25%) and sodium bicarbonate (5%). The chloro-sulfate calcium signature reflects the evolution of the anions of the bicarbonate pole towards the chloride-nitrate pole. This evolution is mainly due to an increase in nitrate, and secondarily by the addition of sulphates in the evolution towards a third facies. Chloride-nitrate water is interpreted as a characteristic of a recently recharged aquifer. On the other hand, the evolution of the waters of the bicarbonate calco-magnesian zone towards the bicarbonate sodium domain could be a sign of some aging of the waters due to the cation exchange indices between alkaline earths and alkalies (Diop and Tijani, 2008).

4.3 Isotopic signal of the local rainfall

The local meteoric waterline (LMWL), based on Niamey's monthly rainfall (Taupin *et al.*, 2003), has the following equation (1992-1999, $n = 28$ and $R^2 = 0.97$):

$$\delta^2\text{H} = 7.7 \delta^{18}\text{O} + 5.4 \quad (1)$$

The slope of this LMWL (7.7) is lower than that of the World Meteorological Water Line (8). This characteristic is interpreted in the Sahel as the result of slightly evaporated precipitation during rainfall, in accordance with the interpretation of the monitoring of isotope concentrations of atmospheric water vapor in Niamey (Tremoy *et al.*, 2012). The origin of precipitation is determined from the values of the deuterium excess:

$$d = \delta^2\text{H} - 8 \delta^{18}\text{O} \quad (2)$$

Tritium concentrations in precipitation show a series of peaks following the first nuclear tests in early 1950's. Current tritium concentrations are of 5 to 10 TU in the precipitation in the northern hemisphere (GNIP, 2011). In southwestern Niger, the most recent measurements were

~7 TU in 1994 and ~4 TU in 2006 (Favreau *et al.*, 2002; Favreau, pers. Com., IRD France, 2016).

The weighted average of the measures, the rainy period number by month, collected in Niger and Burkina Faso between 1998 and 2008 is 5.2 TU (Ousmane, 1988, Favreau *et al.*, 2002, Guéro, 2003, Yaméogo, 2008). This value represents the isotopic signature of the current rains and therefore the input function of the hydrological system. Given the half-life of tritium (12.41 years), groundwater infiltrated before the 1950's (average concentration estimated at 5 TU in precipitation) would have in 2009 (sampling date) a tritium concentration of 0.2 TU, therefore lower than the detection threshold.

4.4 Isotopes in groundwaters

Stable-isotope compositions of 22 groundwater samples, including two samples from wells dug in alterites, range from -4.5 ‰ to +0.9 ‰ for oxygen-18 and -31 ‰ to -0.1 ‰ for deuterium. The overall mean values and standard deviations are respectively -3.0 ‰ and 1.5 ‰ for oxygen-18 and -19 ‰ and 8.2 ‰ for deuterium. Considering only deep bottom aquifers (17 values), mean values of -3.6 ‰ and -23 ‰ for oxygen-18 and deuterium respectively are found. $\delta^{18}\text{O}$ levels are 36% higher than -3 ‰ while 77% have deuterium values lower than -25 ‰. These results highlight the influence of different lithologies and the different groundwater pathways in the area.

The calculated deuterium excess (*d*) values for groundwater are less than 10 (Table 1). This shows that the air masses that generated Niger's precipitation and eventually groundwater recharge originate from the Guinean monsoon, with a marked effect of the re-evaporation of rainfall (Tremoy *et al.*, 2012).

The isotopic composition of groundwater in arid regions can be considerably modified by evaporation in comparison to isotopic composition of the local precipitation (Clark and Fritz 1997, Favreau *et al.*, 2002). However, despite high actual evapotranspiration (AET) values, it

is possible to have groundwater with isotopic compositions close to the average precipitation composition, demonstrating rapid recharge flows to aquifers (Acheamponga and Hess, 2000; Goni, 2006). By plotting the sampled points in the diagram $\delta^2\text{H}$ vs $\delta^{18}\text{O}$ (Figure 6), it is observed that all points are organized around the two following linear regression lines:

$$\delta^2\text{H} = 7.5 \delta^{18}\text{O} + 4.5 \quad R^2 = 0.83 \text{ (Samples from the deep aquifers, } n = 17) \quad (3)$$

$$\delta^2\text{H} = 4.8 \delta^{18}\text{O} - 4 \quad R^2 = 0.95 \text{ (Samples from the shallow aquifers, } n = 5) \quad (4)$$

The 17 points corresponding to the samples taken in the deep aquifers are aligned around line (3) in Fig 6 (expressed by Equation 3) with a slope of 7.6, very close to the slope of the line representative of the local precipitation (LMWL). This suggests rapid recharge to the aquifers without marked evaporation effects as shown in Figures 7, 8 and 9 and confirmed by the computation of the water renewal rate for these aquifers. Three of these boreholes (circled points in Fig 6) deviate from the LMWL and are below the evaporation line (4) in Fig 6 (expressed by Equation 4). This deviation from the LMWL could indicate enrichment by the evaporation process from surface water. The position of these boreholes in the interdunary basins and in sandy zones, which are favorable sites for the concentration of runoff water, the infiltration (Aranyossy and Gaye, 1992; Ngounou Ngatcha *et al.*, 2001) and the evaporation could explain their evaporated intermediate composition. Contrary to the observations made in the neighboring sedimentary zone (Favreau *et al.*, 2002), the deeper part of the aquifers seem to be able to hold slightly evaporated waters. Desconnets *et al.* (1997) show that in the sedimentary zones of the Sahelian regions, ~80 to 90% of the water accumulated in the ponds infiltrate and contribute to the rapid recharge of the aquifers. On the other hand, in the basement area, clayey-sandy alterites have an effect on the infiltration rate due to their low permeability.

Five points are aligned with the straight line (4) in Fig 6, with a slope of 4.8, indicating an enrichment by evaporation of the surface water that supplies the aquifers by the indirect recharge processes (Abdalla, 2009). These five points correspond to wells collecting shallow weathered layers and shallow boreholes screened at the interface between the fractured horizon and grainy weathered horizon. This evaporation line (4) intersects the LMWL through a point of coordinates -4.1 ‰ and -23.1 ‰ corresponding to the mean weighted rainfall composition at the Niamey station. The fact that this point belongs to the evaporation line (2) in Fig 6 indicates that the waters of the shallow aquifers come from the current rains which have undergone evaporation at the surface or in the first meters of the ground. In semi-arid zones, partial evaporation of water in the first meters of the soil is the basis of isotopic enrichment (Edmunds *et al.*, 2002; Stadler *et al.*, 2010).

Tritium activity in the bedrock aquifers shows a wide range of values. The concentrations ranged from <0.9 (detection limit) to 5.9 TU, with an average of 3.69 ± 1.22 TU. Generally speaking, 82% of the Liptako basement groundwater samples have tritium levels of ≥ 3 TU, of which 64% are > 4 TU. This implies that bedrock aquifers contain an important part of the waters that were infiltrated recently, i.e. over the past 50 years. Nevertheless, there are two older water samples with low tritium content (<0.9 TU, 1.4 ± 0.6 TU). High nitrate concentration in this part of the aquifer may be inherited from soil nitrogen sources and subsequent leaching occurring during high recharge events (Schiewede *et al.*, 2005; Favreau *et al.*, 2009).

Waters with tritium levels close to those of recent precipitation (3 to 4.7 ± 0.7 TU) are found in both deep and shallow aquifers. These two levels are distinguished according to their oxygen-18 contents which are relatively enriched in the more shallow aquifers. These shallow aquifers can be characterized by an indirect and rapid mode of recharge through the major bed of koris or laterally by evaporated surface waters.

Thirteen older groundwater samples, within the limits of the Dargol basin and dating back to the early 1980s (Ousmane, 1988), were also considered for an estimate of long-term changes in the renewal rates based on tritium data.

The diagram of $\delta^{18}\text{O}$ vs ^3H highlights the presence of three groups of water belonging to different periods of recharge (Figure 10). Thus, low-tritiated waters (<3 TU) belong to the deeper parts of aquifers characterized by higher oxygen-18 depletion. This older signal could correspond to a recharge during the wetter period of the mid-20th century (B12 <0.9 TU). It may also be interpreted by a slow and diffuse mode of recharge probably induced by rainwater infiltration through the altered zones.

5. Discussion

5.1 Hydrochemical evolution of the groundwater

The hydrogeochemical signature of waters can be used to trace water-aquifer matrix exchanges. An increase in groundwater bicarbonate (and in pH values) results from higher soil CO_2 partial pressure supplied by the infiltration water, assuming there is a closed system in the deeper part of the aquifer. This trend is consistent with the results (see Fig S1 of the ESM) indicating a positive correlation between HCO_3 and $(\text{Na} + \text{K})\text{-Cl}$ in contrast to $(\text{Ca} + \text{Mg})\text{-(HCO}_3 + \text{SO}_4)$ which shows a weaker negative correlation. The latter could be due to the different origins of the Ca^{2+} and Mg^{2+} ions, because the ion exchange reaction supposes the replacement of these ions by Na^+ as a function of aging of the water (see Fig S2 of the ESM). This principle is clearly proved through the diagram $(\text{Na} + \text{K}) - \text{Cl}$ vs $(\text{Ca} + \text{Mg}) - (\text{HCO}_3 + \text{SO}_4)$ made from the points sampled in the dry season. The results of Principal Component (PC) analysis using the same water samples (Abdou Babaye, 2012) show the existence of two main sources of ion production. The first subgroup (Ca^{2+} , NO_3^- , Cl^-) indicates the influence of anthropogenic activities (septic tanks, animal excrement around wells) in the mineralization of water, which is partly confirmed

411 by the presence of NO_3^- (La Vaissière, 2006 ; Diaw, 2008 ; Yaméogo, 2008). It has been shown
412 that the Mg^{2+} , Na^+ , SO_4^{2-} cluster revealed that these ions would come from a different process
413 than pollution through the infiltration of recent waters (Abdou Babaye, 2012). The Mg^{2+} ion in
414 this group shows that some of the waters with a calco-magnesian bicarbonate facies may be
415 associated to old waters (Figure 10).

416 The relationship between Mg^{2+} and $\delta^{18}\text{O}$ clearly discriminates waters of the superficial aquifers
417 from those of the deeper aquifers (Figure 7). This relationship makes it possible to distinguish
418 deep and confined schist aquifers, from granitic aquifers overlaid by sandy clay weathering
419 products more permeable than those found above the schist formations. A clear increase in
420 magnesium content with depth can be observed, except for the boreholes drilled in the granite
421 basement. This increase, and the oxygen-18 among the most depleted in the groundwater
422 samples, would then indicate the relationship between the geochemical process of hydrolysis
423 and the more or less intense water-rock interactions.

424 The saturation index (SI) of calcite and dolomite (Figure 8) and the equilibrium diagram (Figure
425 9) show that the hydrodynamic functioning of these systems is influenced by the lithology of
426 the reservoirs (granitoids, schists, alterites). Thus, recent waters (group 1 in Fig 8), with a high
427 value of pCO_2 and very negative values of the saturation index (sub-saturation), are found in
428 the wells and boreholes close to the Dargol flood plain. In contrast, waters with a longer
429 residence time (group 3 in Fig 8) are found on the plateau, the dunes or in the schist formations
430 overlaid by a thick weathered layer. For the latter, one can deduce a slower circulation rate of
431 the waters with relatively depleted contents of heavy isotopes ($\delta^{18}\text{O} < -4 \text{ ‰}$) and tritium (< 3
432 TU). The isotopic signature of these waters proves that the diffuse recharge is low and that the
433 water resulting from the indirect recharge (from topographic depression) would takes time (\geq
434 50 years based on the lower tritium values) before reaching this part of the aquifer. Regarding
435 the geochemical rock-water interaction (Figure 9), waters are in the stability domains of

kaolinite and montmorillonite. In the equilibrium diagram, this distribution of points is clearly influenced by the lithological nature, or by the distance to the recharge zone. The samples show an evolution from an open environment (groundwater in chemical equilibrium with kaolinite), where groundwaters are less mineralised (granitoid, alterites), towards a confined environment (groundwater more in equilibrium with montmorillonite) as in green rocks with naturally more mineralised waters. Groundwaters are becoming 'older' when passing from the kaolinite equilibrium towards the montmorillonite equilibrium showing confined conditions and probably associated low permeability values. This confinement is mainly related to the thick clayey-sandy alterite layers found in the schists zones, but also to the low-permeability filling of some fractures.

5.2 Recharge rates and changes in groundwater storage

The annual and interannual fluctuations in groundwater levels and the hydrogeochemical behavior of the aquifers reveal the complexity of recharge processes in this semi-arid zone. The litho-tectonic context of the study area accentuates spatial heterogeneity in the hydraulic properties of aquifers due to the variable nature of the weathering products and the degree of fracturation of the surrounding rocks. Variations in groundwater levels are greater in boreholes located at high elevations (plateaux, dunes, rather remote from koris) than in those located in the immediate vicinity of floodplains of koris or ponds (Ousmane , 1988). In schists or dune areas, the characteristics of the land surface results in low diffuse infiltration. The large thickness of the unsaturated zone, the clogging of the ponds and the low infiltration favor the loss of water by evaporation (Figure 11).

These arguments corroborate those suggested by the hydrogeochemical study discussed above. Heavy isotope depletion ($\delta^{18}\text{O} < -4 \text{ ‰}$) and lower tritium content ($< 3 \text{ TU}$) suggest that the aquifers contain a significant component of older water and that recharge by direct infiltration of rainfall is low. The hypotheses on the rate of water renewal are verified by using a simple

analytical model applied in the semi-arid zone (Leduc *et al.*, 2000, Le Gal La Salle *et al.*, 2001, Favreau *et al.*, 2002) where the water renewal rate is high. This model makes it possible to calculate not only renewal rates in 2009 but also possible changes since the early 1980s (Table 2). Thus, the following equation can be used to calculate the average tritium content in an aquifer in a year i :

$$Av_i = (1 - Tr_i)Av_{i-1}e^{-\left(\frac{\ln 2}{T}\right)} + Tr_iAp_i \quad (5)$$

Where Tr_i is the renewal rate of the water in the aquifer, T the half-life of tritium (12.43 years) and Ap_i the tritium content in precipitation for the year i .

Given the uncertainties associated with the recharge and tritium concentration in the recharge, and the possible variations in pumping or volume of the aquifer, the only significant variations between 1980-1981 and the end of 2009 are observed for the wells Sirfikouara (B19) and Toumbindé B7) with respectively 2 and 3 times the renewal rate. The aquifer remained stable at wells B20 and B21. The proximity of these wells (B19, B20, B21) to the riverbed of the Koris and especially the permeability of the shallow weathered materials (sands and granitic sand) facilitate the infiltration of water on the one hand, but also the direct hydraulic relationship between the superficial and deep aquifers on the other hand. This is highlighted on the cross-section AB (Figures 3 and 12) showing the hydraulic equilibrium between these two superimposed aquifers, contrary to the phenomenon observed in schists formations (cf. Figure 11).

In the Yanga area (B12; Figure 11), an apparent decrease in the renewal rate is observed. The exceptional characteristics of waters sampled in B12 are mainly their high mineralization ($> 1100 \mu\text{S/cm}$) but also their tritium content below the detection limit ($< 0.9 \text{ TU}$). These samples also belong to the family of waters close to saturation (cf Figure 8) corresponding to confined aquifers, with slow transit time leading to a low renewal rate or even no renewal during the years of drought. All these elements suggest that these waters have infiltrated very rapidly in a

more humid period and at a lower temperature than that of the current climate. This is consistent with the theory of mixing of water of ancient origin prior to 1954 (Girard *et al.*, 1997), as suggested by Ousmane (1988) from the activities of ^{14}C .

The results of the model do not show a clear trend in the evolution of the aquifer renewal rate or in the storage in the aquifer (see Figure 3). Comparison of renewal rates computed on the long-term is appropriate for groundwaters (Mc Donnell, 2017); the median value of individual renewal rates of the 1980-1981 data set of groundwater tritium is of 20 % decade⁻¹, an estimate that can be considered close, considering the high interannual variability in recharge in the Sahel (Favreau *et al.*, 2009), to the one inferred (13% decade⁻¹) from the groundwater sampling and analyses performed in 2009, approximately three decades later.

Table 2: Comparison of tritium content in boreholes in 1980-1981 (in Ousmane, 1988) and 2009 (this study).

Locality	Ousmane (1988)		This study		Renewal rate in 1980 (% y ⁻¹)	Renewal rate in 2009 (% y ⁻¹)
	Tritium (TU)	Date	Tritium (TU)	Date		
Sirfikouara (B19)	8.1±2.4	23/10/1980	4.1±0.8	01/11/2009	0.44	1.25
Tera camp (B20)	15	17/06/1981	3.6±1.1	31/10/2009	0.86	1.0
Tera pont (B21)	15	16/06/1981	3±0.5	31/10/2009	0.86	0.78
Toumbindé (B7)	15	24/10/1980	4.7±0.7	27/10/2009	0.86	1.60
Yanga (B12)	41±7	24/10/1980	< 0.9	25/10/2009	3.3	<0.2
Dam	15	19/03/1981	5.2±0.8	18/12/2009	-	-
Rainfall	15*	31/08/1980	5.21**	1998-2008	-	-

(*)Niamey-Université station,

(**) Mean tritium concentration in rainfall (period 1998-2008; Dosso and Niamey stations) and from Burkina Faso (Ouagadougou station).

5.3 Recharge conceptual model

504 Understanding the different recharge processes is an essential step for further assessment of the
505 hydrodynamic functioning of the aquifers. Studies on the recharge mechanisms in arid and
506 semi-arid environments in Africa have shown the importance of the drainage network in this
507 process (Desconnets *et al.*, 1996, Leduc *et al.*, 1996a). Temporary watercourses and endorheic
508 pools can constitute preferential recharge zones. In basement areas, the concordance between
509 the hydrographic network and the main tectonic fractures could enable a preferential infiltration
510 towards the deep basement (Rana, 1998).

511 The spatial distribution of tritium contents (Figure 3) shows that the groundwater with high
512 tritium concentrations is located near the koris beds. The tritium content in groundwater also
513 decreases as the distance of the sampling points to the topographic depressions zones increases.
514 Two assumptions could be invoked for explaining the presence of older waters in the upper
515 areas. One could argue that the recharge occurs by direct diffuse percolation of the rain through
516 the variably saturated zone. Its relative low permeability would explain long travel times. This
517 is however unlikely the case considering the large thickness over the saturated zone and the dry
518 conditions favoring evaporation of the infiltrated waters (Favreau *et al.*, 2002). Moreover, some
519 observations are in contradiction with this hypothesis showing a current isotopic signature
520 despite the thickness and low permeability of the overlying cover (see Figure 8). In the
521 basement area, groundwater flow is generally influenced by the density of fractures, but
522 especially by the deep fractures which constitute the preferential pathways for groundwater.
523 This leads to the second hypothesis, which states that major fractures are the preferential
524 pathways for the rapid drainage of recharge waters. Thus, recent waters are found in boreholes
525 screened in major fractures, while old waters are located in less permeable areas characterized
526 by secondary fractures (Diop and Tijani, 2008). Ousmane (1988) showed that the isotopic
527 contents of the Sahelian basement water generally show a significant heterogeneity since each
528 isolated fracture constitutes a distinct aquifer system recharged locally by vertical infiltration.

529 In the Kobio basin, located about 100 km south-east of Tera (see Figure 1), Girard *et al.* (1997)
530 have highlighted the importance of the fracture network in the recharge process, but also the
531 continuity of the aquifer due to the fracture network density.

532 The interconnection of fractures and the permeability of filling materials locally determine the
533 continuity of the aquifer (Ball *et al.*, 2010). However, the boreholes may belong to different
534 hydraulic systems, isolated by fractures filled by clays acting as a low-permeability barrier
535 (Ousmane *et al.*, 1983). The low tritium (below the detection limit) and low heavy isotope ($\delta^{18}\text{O}$
536 of -7.4 ‰) content are related to the litho-structural context and to the recharge mechanism of
537 the upper zones (Girard *et al.*, 1997). These were demonstrated by the results of the present
538 study through the isotopic heterogeneity accentuated by the hydraulic discontinuity due to the
539 faults which do not favor the continuity of circulation of water beyond this zone (Ousmane,
540 1988, Nkotagu, 1996). The boreholes (B1, B11) located along the NE-SW major fault where
541 the Tilim River flows show an isotopic homogeneity (^{18}O and ^3H); whereas those located on
542 either side of this fault show different isotopic signatures (see Figure 8, Figure 3). These very
543 close boreholes capture different fractures, fractures connected to the major fault with recent
544 waters due to rapid and recharge, and secondary fractures with isolated old waters (Diop and
545 Tijani, 2008). The non-connection of the latter with the major fractures and the drainage
546 network give these waters specific isotopic signatures. Thus, these fractures can only receive
547 water from vertical infiltration with transit times up to 30-60 years under fallow soils in arid
548 regions (Ibrahim *et al.*, 2014). According to Lapworth *et al.*, (2013), the transit time through
549 the unsaturated zone can reach 100 years in semi-arid regions. This delay may, however be
550 shortened by the low thickness of the unsaturated zone or the high conductivity of fractures
551 (Stadler *et al.*, 2010) leading to a very short transit time.

552 It should be noted that in basement areas of humid regions, stable-isotope compositions are
553 relatively homogeneous in fractured aquifers due to the high precipitation and water stock in

the unsaturated zone (Adiaffi *et al.*, 2009; Lapworth *et al.*, 2013). This zone acts as a buffer to homogenise by mixing the successive infiltration waters and minimise the chemical heterogeneity in the saturated zone (Lapworth *et al.*, 2013). The spatial heterogeneity of the isotopic composition of groundwater in arid and semi-arid regions (Leduc *et al.*, 1997, Le Gal La Salle *et al.*, 2001) is due to the spatial and temporal variations of the recharge. In addition, rainfall events from the core of the rainy season (mid-July – mid-September) are known to usually result in more depleted values in their stable isotopic composition (Ousmane, 1988; Goni *et al.*, 2001; Taupin *et al.*, 2002, 2003; Favreau *et al.*, 2002; Saravana *et al.*, 2009; Massing and Tang, 2010). Processes favoring infiltration during those periods could influence the groundwater isotopic composition.

5.4 Impact of vegetation cover and climate variability

Several studies carried out in arid zones have demonstrated the influence of climatic variability and changes in vegetation cover on water resources (Leduc *et al.*, 2001, Favreau *et al.*, 2009, Ibrahim *et al.*, 2014). In Niger, degradation of vegetation cover and increase in growing areas have resulted in an increase in runoff, despite a decline of about 20% in annual rainfall (Taylor *et al.*, 2002). Thus, the global runoff coefficient (i.e. ratio between total rainfall and measured total runoff at a discharge point of the considered basin) calculated on the Dargol at Tera has increased from 6.2% (before 1972) to 8.4% over the period from 1972 to 1992. Soil crusting and closure of macropores partly explain the predominance of localized recharge, leading to an increase in groundwater levels in the immediate vicinity of watercourses in the Continental Terminal (CT) aquifer (Favreau *et al.*, 2002), ~150 km east of the study area. This process could explain the large increase in the groundwater level observed in the boreholes (W1 and B9; Figure 4) localised in topographic depressions. Contrary to the observation made in the sedimentary areas, basement aquifers generally show a piezometric decline since the early 1980s (Figure 4). For the Burkina-Faso basement area, Filippi *et al.* (1990) showed that the

decrease in rainfall results in a decrease in groundwater levels. The sensitivity of the aquifers to rainfall fluctuations is due to the rapid mode of recharge through open fractures on the one hand and to the low capacity of soil aquifers to store a lot of water on the other hand. These distributions distinguish them from regional sedimentary aquifers, where renewal rates are usually much lower ($< 0.1\% \text{ a}^{-1}$ in the CT aquifer in SW Niger; Favreau *et al.*, 2002) that can more easily mitigate the effect of climate change.

6. Conclusion

The combined interpretation of groundwater level and hydrogeochemical data provided new insights into the hydrodynamic functioning and recharge processes of the fissured and weathered aquifers of southwestern Niger. The shallow aquifers of alterites are unconfined, whereas those of the fissured and / or fractured basement are often confined. The degree of confinement of these layers depends on the covering materials that are genetically related by weathering to the type of bed-rock. Thus, the permeability of the alteration products of the granitic rocks allows a good interaction (and therefore without confinement) between the superficial and deep aquifers. On the other hand, the less permeable clayey alteration above the schist aquifers creates confined conditions in these aquifers. The chemical and isotopic data have provided useful information to trace the path followed by infiltration water and their residence time in aquifers. Thus, the origin and the recharge processes, and the transit time of the waters have been specified. The main conclusions drawn from this study can be summarized as follows:

- The distribution of isotopic contents in groundwater shows spatial variations accentuated by the hydraulic discontinuity due to fractures. These variations confirm a relative independence of each fracture in the groundwater circulation.
- The recharge of the aquifers follows two distinct mechanisms: a direct recharge from the precipitation that does not undergo significant evaporation for the majority of the boreholes,

and an indirect recharge from highly evaporated surface water found in the wells getting water from the alterite or shallow aquifers;

- Tritium contents confirm an important component of recent waters, which, given the depth of the screen depths (20 to 120 m), implies rapid infiltration through fractures or major faults superimposed on the surface drainage network. In the groundwater sector where tritium concentrations are < 3 TU, the renewal rate may be lower. The evolution of radioactive decay in the waters of the boreholes sampled at the beginning of the 1980s provides further details on the role of diffuse infiltration in the recharge of the waters but also on the mixing process and changes in the renewal rate, and recharge on a pluri-decennial scale.
- The water-rock interaction, through the saturation index and the equilibrium diagrams of the minerals, allowed to estimate the approximate age of the water and to distinguish the parts of the aquifers where the recharge is weak.

This study proves that the aquifer system is well connected to the land surface through the fracture system. In addition to the low hydraulic conductivity and storativity of these aquifers, this means that the aquifers are very sensitive both to drought and pollution. A long drought resulting from climate change could result in dramatic decline in water level and well drying. The potential impact of agricultural and industrial development on groundwater quality is also immediate and huge. As a result, protection against contamination remains a major challenge. Taking into account these two problems is thus of primary importance for the management of these groundwater resources.

Acknowledgments

This study was funded by the Belgian Technical Cooperation (BTC), the University of Liège (ULg) and by The International Foundation for Science (IFS grant, 2008). Some technical support was also provided by the AMMA-Catch team at IRD in Niger. This would not have happened without the logistical help of AbdouMoumouni University (UAM) and we express our deep gratitude to them.

References

- Abdalla O. A. E. (2009) Groundwater recharge/discharge in semi-arid regions interpreted from isotope and chloride concentrations in north White Nile Rift, Sudan. *Hydrogeol. J.*, 17, 679–692. DOI 10.1007/s10040-008-0388-9.
- Abdou A., Bonnot H., Bory K. D., Chalamet D., St Martin M., Younfa I. (1998) Notice explicative des cartes géologiques du Liptako à 1/100 000 et 1/200 000. [Explanatory note of the geological maps of the Liptako region at scales of 1/100,000 and 1/200,000]. Ministry of Mines and Energy, Niger Republic, 64 p.
- Abdou Babaye M. S. (2012) Evaluation des ressources en eau souterraine dans le bassin de Dargol (Liptako – Niger). [Groundwater resources estimates in the River Dargol basin (Liptako, Niger)]. PhD Thesis Univ. Liège, 235p.
- Acheamponga S. Y., Hess J. W. (2000) Origin of the shallow groundwater system in the southern Voltaian Sedimentary Basin of Ghana: an isotopic approach. *J. Hydrol.*, 233, 37-53.
- Adiaffi A., Marlin C., Oga Y. M. S., Massault M., Noret A., Biemi J. (2009) Palaeoclimatic and deforestation effect on the coastal fresh groundwater resources of SE Ivory Coast from isotopic and chemical evidence. *J. Hydrol.*, 369, 130 –141.
- Affaton P., Gaviglio P., Pharissat A. (2000) Réactivation du craton ouest-africain au Panafricain : paléocontraintes déduites de la fracturation des grès néoprotérozoïques de KareyGorou (Niger, Afrique de l’Ouest). [Reactivation of the West-African craton during the Panafrican

653 tectonic cycle: evidence of paleostresses recorded by brittle deformation in the
654 Neoproterozoic sandstones of KareyGorou (Niger, West Africa)].C. R. Acad. Sci. Paris,
655 Sciences de la Terre et des planètes, 331, 609–614.

656 Aggarwal, P. K., Gat J. R. and K. F. O Froehlich (eds) (2005) Isotopes in the water cycle: past,
657 present and future of a developing science. IAEA, Dordrecht NL: Springer.

658 Amani A., Nguetora M. (2002) Evidence d’une modification du régime hydrologique du fleuve
659 Niger à Niamey. [Evidence of a change in the hydrological regime of the River Niger in
660 Niamey]. IAHS Publ. 274; 449-456

661 Aranyossy J. F., Gaye C. B. (1992) Use of the tritium thermonuclear peak in the deep
662 unsaturated zone for quantitative estimate of aquifer recharge under semiarid conditions –
663 First application in the Sahel. C.R. Acad. Sci. Paris 315 (ser II) : 637-643

664 Bajjali W. (2008) Evaluation of groundwater in a three-aquifer system in Ramtha area, Jordan:
665 recharge mechanisms, hydraulic relationship and geochemical evolution. Hydrogeol. J. 16,
666 1193–1205.

667 Ball L. B., GE S., Caine J. S., Revil A., Jardani A. (2010) Constraining fault-zone hydrogeology
668 through integrated hydrological and geoelectrical analysis. Hydrogeol. J., 1057–1067.

669 Bouragba L., J.Mudry J., Bouchaou L., Hsissou Y., Krimissa M., Tagma T., Michelot J. L.
670 (2011) Isotopes and groundwater management strategies under semi-arid area: Case of the
671 Souss upstream basin (Morocco). Applied Radiation and Isotopes 69 (2011) 1084–1093.

672 Carrillo-Rivera J. Joel, Clark I. D., Fritz Peter (1992) Investigating recharge of shallow and
673 paléo-groundwaters in the villa de Reyes basin, SLP, Mexico, with environmental isotopes.
674 Applied Hydrogeology 4, 35-48.

675 Clark, I. D. (2015) Groundwater geochemistry and isotopes. Boca Raton: CRC Press Taylor &
676 Francis Group.

677 Cook, P., Dogramaci, S., McCallum, J. and J. Hedley (2017) Groundwater age, mixing and
678 flow rates in the vicinity of large open pit mines, Pilbara region, northwestern Australia.
679 Hydrogeol. J. 25, 39-53.

680 Dakoure D. (2003) Etude hydrogéologique et géochimique de la bordure sud-est du bassin
681 sédimentaire de Taoudeni (Burkina Faso - Mali) - essai de modélisation [Hydrogeological
682 and geochemical study of the southeastern part of the Taoudenisedimentary basin (Burkina
683 Faso - Mali) – first modeling attempt]. PhD thesis, Univ. Paris VI - Pierre et Marie Curie,
684 223p.

685 De La Vaissière R. (2006) Etude de l'aquifère néogène du Bas-Dauphiné. Apports de la
686 géochimie et des isotopes dans le fonctionnement hydrogéologique du bassin de Valence
687 (Drôme, Sud-Est de la France) [Study of the Neogene aquifer of the lower Dauphiné region.
688 Contribution of geochemistry and isotopes approaches in the hydrogeological functioning
689 of the Valence basin (Drôme, southeastern France)]. PhD thesis, University of Avignon
690 and the Vaucluse region, 339p.

691 De Vries J. J., Simmers I. (2002) Groundwater Recharge: an overview of processes and
692 challenges. Hydrogeol. J., 1, 5-17.

693 Desconnets J. C., Taupin J. D., Lebel T, Leduc C. (1997) Hydrology of the Hapex-Sahel Central
694 super-site: surface water drainage and aquifer recharge through the pool systems. J. Hydrol.
695 188:155–178.

696 Dewandel B., Lachassagne P., Wyns R., Maréchal J. C., Krishnamurthy N. S. (2006) A
697 generalized 3-D geological and hydrogeological conceptual model of granite aquifers
698 controlled by single or multiphase weathering. J. Hydrol. 330, 260-284.

699 Diaw M. (2008) Approche hydrochimique et isotopique de la relation eau de surface/nappe et
700 du mode de recharge de la nappe alluviale dans l'estuaire et la basse vallée du fleuve
701 Sénégal : Identification des zones inondées par Télédétection et par traçage isotopique.

702 [Hydrodynamics and isotopic approaches of the relationships between surface and
703 groundwaters and of the recharge processes of the alluvial aquifer in the downstream part
704 of the Senegal River: identifying flooded areas by remote sensing and isotopic tracers] PhD
705 thesis, Univ. C.A. Dakar, 178p.

706 Diop S, Tijani M. N. (2008) Assessing the basement aquifers of Eastern Senegal. *Hydrogeol.*
707 *J.* 16:1349–1369, DOI 10.1007/s10040-008-0353-7

708 Dupuis D., Pons J., Prost A.E. (1991) Mise en place de plutons et caractérisation de la
709 déformation birimienne au Niger occidental. [Plutonic emplacement and Birimian
710 deformation in western Niger]. *C.R. Acad. Sci. Paris*, 312 (II), 769 – 776.

711 Edmunds W.M., E. Fellman, I.B. Goni et C. Prudhomme (2002) Spatial and temporal
712 distribution of groundwater recharge in northern Nigéria. *Hydrogeol. J.*, 10, 205-215.

713 Favreau, G., B. Cappelaere, S. Massuel, M. Leblanc, M. Boucher, N. Boulain, and C. Leduc
714 (2009) Land clearing, climate variability, and water resources increase in semiarid
715 southwest Niger: A review, *Water Resour. Res.*, 45, W00A16,
716 DOI:10.1029/2007WR006785.

717 Favreau G., Leduc C., Marlin C., Guero A. (2002) A rising piezometric depression in the Sahel
718 (southwestern Niger). *C. R. Geoscience* 334, 395–401.

719 Favreau G., Nazoumou Y., Leblanc M, Guéro A., Goni I. B. (2012) Groundwater ressources
720 increase in the Iullemmeden Basin, West Africa. *IAH – Inter. Contr. To Hydrogeo.*, 27,
721 113-128.

722 Filippi, C., Milville, F., Thiery, D., (1990) Evaluation of natural recharge to aquifers in the
723 Sudan-Sahel climate using global hydrological modelling: application to ten sites in
724 Burkina Faso. *Hydrol. Sci. J.*, 35, 29-48.

725 Gardelle J., Hiernaux P., Kergoat L., Grippa M. (2010) Less rain, more water in ponds: a remote
 726 sensing study of the dynamics of surface waters from 1950 to present in pastoral Sahel
 727 (Gourma region, Mali). *Hydrol. Earth Syst. Sci.*, 14, 309–324.

728 Gaultier, G. (2004) Recharge et paléorecharge d'une nappe libre en milieu sahélien (Niger
 729 Oriental) : approches géochimique et hydrodynamique. [Recharge and paleorecharge of a
 730 superficial aquifer in the Sahel (southeast Niger): geochemistry and hydrodynamic
 731 approaches]. PhD thesis, Univ. Paris Sud, 179p.

732 Girard P. (1993) Techniques isotopiques (^{15}N , ^{18}O) appliquées à l'étude des nappes des
 733 altérites et du socle fracturé de l'ouest africain. Étude de cas: l'Ouest du Niger. [Isotopic
 734 techniques (^{15}N , ^{18}O) applied for groundwater in alterites and hard rock aquifers of West
 735 Africa. Case study: West Niger] PhD thesis, Univ. Québec à Montréal, 141p.

736 Girard P., Hillaire-Marcel C., Oga M.S. (1997) Determining the recharge mode of Sahelian
 737 aquifers using water isotopes. *Journal of Hydrology*, n° 197, 189–202.

738 GNIP (2011) Global Network of Isotopes in Precipitation. [http://www-](http://www-naweb.iaea.org/napc/ih/IHS_resources_isohis.html)
 739 [naweb.iaea.org/napc/ih/IHS_resources_isohis.html](http://www-naweb.iaea.org/napc/ih/IHS_resources_isohis.html), last access January 2018

740 Goni I. B. (2006) Tracing stable isotope values from meteoric water to groundwater in the
 741 southwestern part of the Chad basin. *Hydrogeol. J.* 14: 742–752.

742 Goni I.B., Fellman, Edmunds W.M (2001) Rainfall geochemistry in the Sahel region of
 743 northern Nigeria. *Atmospheric Environment*, 35, 4331-4339.

744 Guéro A. (2003) Étude des relations hydrauliques entre les différentes nappes du
 745 complexe sédimentaire de la bordure sud-ouest du bassin des Iullemmeden (Niger) :
 746 approches géochimique et hydrodynamique [Study of hydraulic relationships between the
 747 different aquifers of the sedimentary complex of the southwestern border of the
 748 Iullemmeden basin (Niger): hydrodynamics and geochemical approaches]. PhD Thesis,
 749 Univ. Paris XI Orsay, 265 p.

Ibrahim M., Favreau G., Scanlon B. R., Seidel I. C., Le Coz M., Demarty J., Cappelaere B. (2014) Long-term increase in diffuse groundwater recharge following expansion of rainfed cultivation in the Sahel, West Africa. *Hydrogeol. J.*, DOI 10.1007/s10040-014-1143-z

INS (2012) Présentation des résultats préliminaires du quatrième recensement général de la population et de l'habitat (RGP/H) [Presentation of the preliminary results of the 4th general census of the population and living conditions (RGP/H)]. Niger Republic, 9p.

Lapworth D.J., MacDonald A. M., Tijani M. N., Darling W. G., Gooddy D. C., Bonsor H. C., L. J. Araguás-Araguás L. J. (2012) Residence times of shallow groundwater in West Africa: implications for hydrogeology and resilience to future changes in climate. *Hydrogeol. J.* 21: 673–686, DOI 10.1007/s10040-012-0925-4.

Leblanc M., Favreau G., Massuel S., Tweed S., Loireau M., Cappelaere B. (2008) Land clearance and hydrological change in the Sahel: SW Niger. *Global and Planetary Change* GLOBAL-01298

Leblanc M., Tweed S., Van Dijk A., Timbal B. (2012) A review of historic and future hydrological changes in the Murray-Darling Basin. *Global and Planetary Change* 80–81, 226–246

Leduc C., Favreau G., Schroeter P. (2001) Long-term rise in a Sahelian water-table: the continental terminal in south-west Niger. *J. Hydrol* 243: 43–54.

Leduc C., Sabljak S., Taupin J-D., Marlin C., Favreau G. (2000) Estimation de la recharge de la nappe quaternaire dans le Nord-Ouest du bassin du lac Tchad (Niger oriental) à partir de mesures isotopiques. [Recharge of the Quaternary water table in the northwestern Lake Chad basin (southeastern Niger) estimated from isotopes]. *C.R. Acad. Sci. Paris*, n° 330, 355–361.

Leduc C., Taupin J-D., Le Gal La Salle C. (1996) Estimation de la recharge de la nappe phréatique du Continental Terminal (Niamey, Niger) à partir des teneurs en tritium.

775 [Recharge of the Continental Terminal water-table (Niamey, Niger) estimated from tritium
776 measurements and modelling]. C.R. Acad. Sci. Paris, t. 323, série II a, 599-605.

777 Le Gal La Salle C., Marlin C., Leduc C., Massault M., Favreau G. (2001) Renewal rate
778 estimation of groundwater based on radioactive tracers (^3H et ^{14}C) in an unconfined aquifer
779 an a semi-arid area, Iullemede Basin, Niger. J. Hydrol., 254, 145– 156.

780 L'Hôte Y., Mahé G., Some B., Triboulet J. P. (2002) Analysis of a Sahelian annual rainfall
781 index from 1896 to 2000; the drought continues. Hydrological Science, 47, 56 –572.

782 Machens E. (1973) Contribution à l'étude des formations du socle cristallin et de la couverture
783 sédimentaire de l'Ouest de la République du Niger. Mémo. (Contribution to the study of
784 the formations of the crystalline basement and the sedimentary cover of the West of the
785 Republic of Niger. Memo.) BRGM, n°82, 167p

786 Mahé G. (2009) Surface/groundwater interactions in the Bani and Nakambe rivers, tributaries
787 of the Niger and Volta basins, West Africa. Hydrol.Sci., 54(4), 704-712.

788 Mahé G., Leduc C., Amani, A., Paturel J.E., Girard S., Servat E., Dezetter A. (2003).
789 Augmentation récente du ruissellement de surface en région soudano-sahélienne et impact
790 sur les ressources en eau [Recent increase in runoff in the Sudano-Sahelian region and its
791 impact on water resources]. In: Hydrology of Mediterranean and Semiarid Regions. IAHS
792 Pub. 278, 215-222.

793 Massing O., Tang Z. (2010) Recharge of the Quaternary Aquifer of Lake Chad Basin
794 Estimated from Oxygen-18 (^{18}O) and Tritium (^3H) Isotopes. Journal of American Science,
795 6 (9), 283-292.

796 McDonnell J. (2017) Beyond the water balance. Nat. Geosci. Vol. 10.
797 www.nature.com/naturegeoscience. Accessed 2017

798 NgounouNgatcha B., Mudry J., Wakponou A., Ekodeck G.E., Njitchoua R., Sarrot-Reynaul
799 J. (2001) Le cordon sableux Limani-Yagoua, extrême-nord Cameroun, et son

800 rôlehydraulique (The Limani-Yagoua sandy belt, far north Cameroon, and its hydraulic
801 role.). *Journal of African Earth Sciences*, 32(4), 889-898.

802 Nicholson S.E. (2001) Climatic and environmental change in Africa during the last two
803 centuries. *Clim Res*, 17, 123–144.

804 Nkotagu (1996) Origins of high nitrate in groundwater in Tanzania. *Journal of African Earth*
805 *Sciences*. 21(4),. 471-478.

806 Ousmane B. (1988) Étude géochimique et isotopique des aquifères du socle de la bande
807 sahélienne du Niger (Liptako, Sud-Maradi, Zinder-Est). [Geochemical and isotopic study
808 of the basement aquifers of the Sahelian belt of Niger (Liptako, South Maradi, East Zinder].
809 PhD thesis, Univ. Niamey, 175p.

810 Ousmane, B., Fontes J. C., Aranyossy J. F., Joseph A. (1983) Hydrologie isotopique et
811 hydrochimie des aquifères discontinus de la bande sahélienne et de l'Aïr (Niger)' [Isotope
812 hydrology of the discontinuous aquifers of the Sahelian belt and the Aïr (Niger)]. In:
813 *Isotope hydrology, 1983, IAEA Vienna*, 367-395.

814 Ousmane B., Galadima S., Moumouni A., Soumana I. (2012) La qualité physico-chimique
815 des eaux des aquifères discontinus du socle du Département de Téra (Liptako, Niger) :
816 impacts sur les taux de desserte en eau potable des populations rurales au sahel. [Physico-
817 chemical quality of water in basement discontinuous aquifers of the department of Tera
818 (Liptako, Niger): impacts on the drinkable water supply rates in Sahel rural areas]. *Africa*
819 *Geosci. Review*, 19(1), 1-16

820 Panthou G., Vischel T., Lebel T. (2014) Recent trends in the regime of extreme rainfall in the
821 Central Sahel. Short Communication. *Int. J. Climatol.* 34: 3998–4006. DOI:
822 10.1002/joc.3984

823 Rana S. S. (1998) Application of Directional Filtering in Lineament Mapping for Groundwater
824 Prospecting Around Bhinmal – A Semi Arid Part of Thar Desert. Jour. Indian Society of
825 Remote Sensing, 26 (1-2), 35-44.

826 Sagna P., Ndiaye O., Diop C., Niang A. D., Sambou P. C. (2015) Les variations récentes du
827 climat constatées au Sénégal sont-elles en phase avec les descriptions données par les
828 scénarios du GIEC ? [Are recent climate variations observed in Senegal in conformity with
829 the descriptions given by the IPCC scenarios?] Pollution atmosphérique, 227, 1-17.

830 Saravana K. U., Suman S., Navada S.V., Deodhar A.S. (2009) Environmental isotopes
831 investigation on recharge processes and hydrodynamics of the coastal sedimentary aquifers
832 of Tiruvadanai, Tamilnadu State, India. J. Hydrol, 364, 23– 39.

833 Scanlon B. R., Keese K. E., Flint A. L., Flint L. E., Gaye C. B., Edmunds W. M., Simmers I.
834 (2006) Global synthesis of groundwater recharge in semiarid and arid regions.
835 Hydrol.Process. 20, 3335–3370.

836 Schiewede M., Duijnisveld W. H. M., Böttcher J. (2005) Investigation of processes leading to
837 nitrate enrichment in soils in the Kalahari Region, Botswana. Physics and Chemistry of the
838 Earth 30, 712-716.

839 Séguis, L., B. Cappelaere, G. Milesi, C. Peugeot, S. Massuel, and G. Favreau (2004)
840 Simulated impacts of climate change and land-clearing on runoff from a small Sahelian
841 catchment, Hydrol. Processes, 18, 3401–3413, doi:10.1002/hyp.1503.

842 Solder, J. E., Stolp, B. J., Heiweil, V. M. and D. D. Susong (2016) Characterization of mean
843 transit time at large springs in the Upper Colorado River Basin, USA: a tool for assessing
844 groundwater discharge vulnerability. Hydrogeology Journal 24, 2017-2033.

845 Soumaila A., Konate M. (2005) Caractérisation de la déformation dans la ceinture birimienne
846 (paléoprotérozoïque) de Diagorou-Darbani (Liptako nigérien, Afrique de l'Ouest)

847 [Characterization of the deformation in the Birimian belt (Paleoproterozoic) of the
848 Diagorou-Darbani (Niger Liptako, West Africa)]. *Africa Geosc. Rev.*, 12(3), 161-178.

849 Stadler S., Osenbrück k., Suckow A.O., Himmelsbach T., Hötzl H. (2010) Groundwater flow
850 regime, recharge and regional-scale solute transport in the semi-arid Kalahari of Botswana
851 derived from isotope hydrology and hydrochemistry. *J. Hydrol.*, 388, 291–303.

852 Taupin J-D, Gaultier G., Favreau G., Leduc C., Marlin C. (2002) Variabilité isotopique des
853 précipitations sahéliennes à différentes échelles de temps à Niamey (Niger) entre 1992 et
854 1999 : implication climatique. [Isotopic variability of Sahelian rainfall at different time
855 steps in Niamey (Niger, 1992–1999): climatic implications]. *C. R. Geoscience*, 334, 43–
856 50.

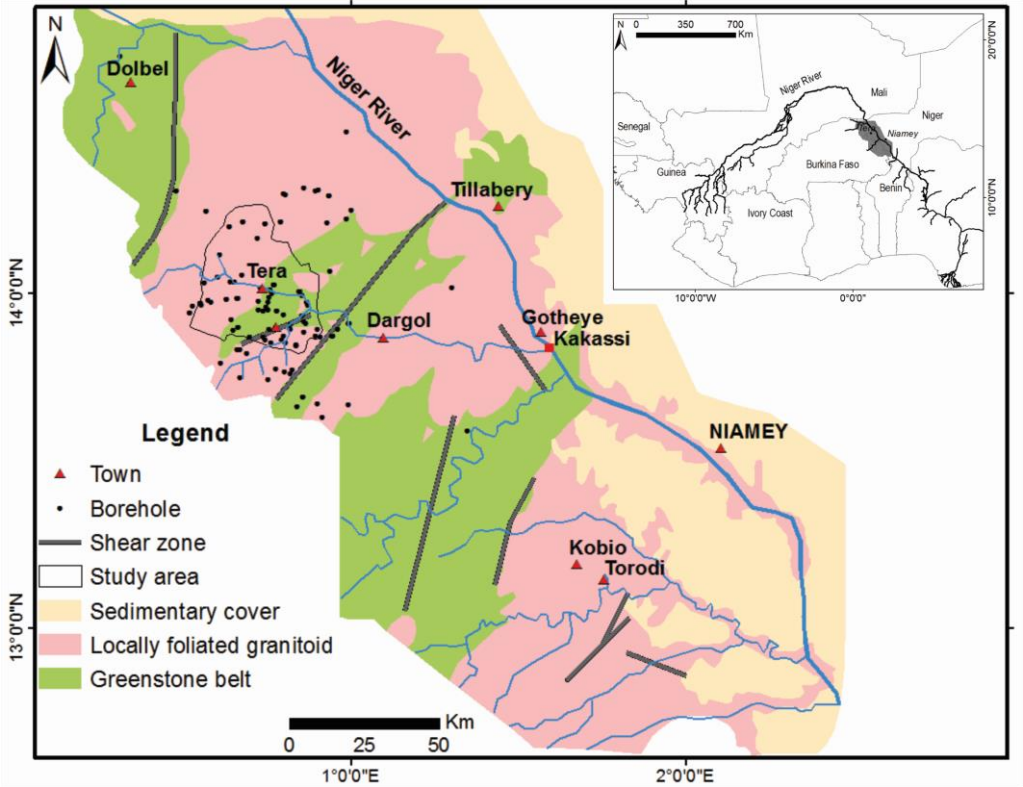
857 Taupin J-D, Gaultier G., Favreau G., Leduc C., Ramirez E. (2003) Étude isotopique des
858 précipitations sahéliennes à l'échelle de l'événement: relation avec les paramètres
859 météorologiques et le type de précipitation [Isotopic study of Sahelian rainfall at the event
860 scale: relationship with meteorological parameters and rainfall characteristics]. *Hydrology
861 of the Mediterranean and Semiarid Regions*, IAHS, 278, 179-185.

862 Taylor C, Lambin E, Stephenne N, Harding R, Essery R (2002) The influence of land use
863 change on climate in the Sahel. *J Climate*, 15, 3615–3629

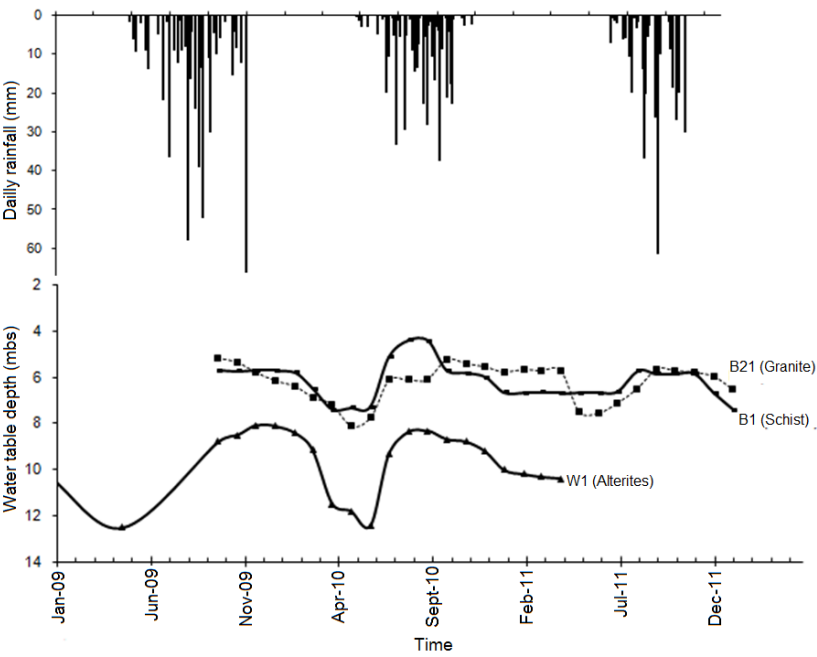
864 Tremoy G., Vimeux F., Mayaki S., Souley I., Cattani O., Risi C., Favreau G., Oï M. (2012) A
865 1-year long $d^{18}O$ record of water vapor in Niamey (Niger) reveals insightful atmospheric
866 processes at different timescales. *Geophysical Research Letters*, 39, L08805,
867 doi:10.1029/2012GL051298, 5p.

868 Yaméogo O. S. (2008) Ressources en eau souterraine du centre urbain de Ouagadougou au
869 Burkina Faso, qualité et vulnérabilité. [Groundwater resources in the urban center of
870 Ouagadougou in Burkina-Faso, quality and vulnerability]. PhD Thesis, University of
871 Avignon and the Vaucluse region, Univ. Ouagadougou, 245p.

872 FIGURES :



873
874 **Fig. 1** Location and geological context of the study area (Adapted from Dupuis *et al.*, 1991)
875 within the Niger River Basin in West Africa (inset).



876
877 **Fig. 2** Fluctuations in the depth to the water table in the shallow aquifer (W1) and in the deep
878 fractured aquifer (B1, B21; see fig. 11 and fig. 12). Daily rainfall measured at the Tera station.

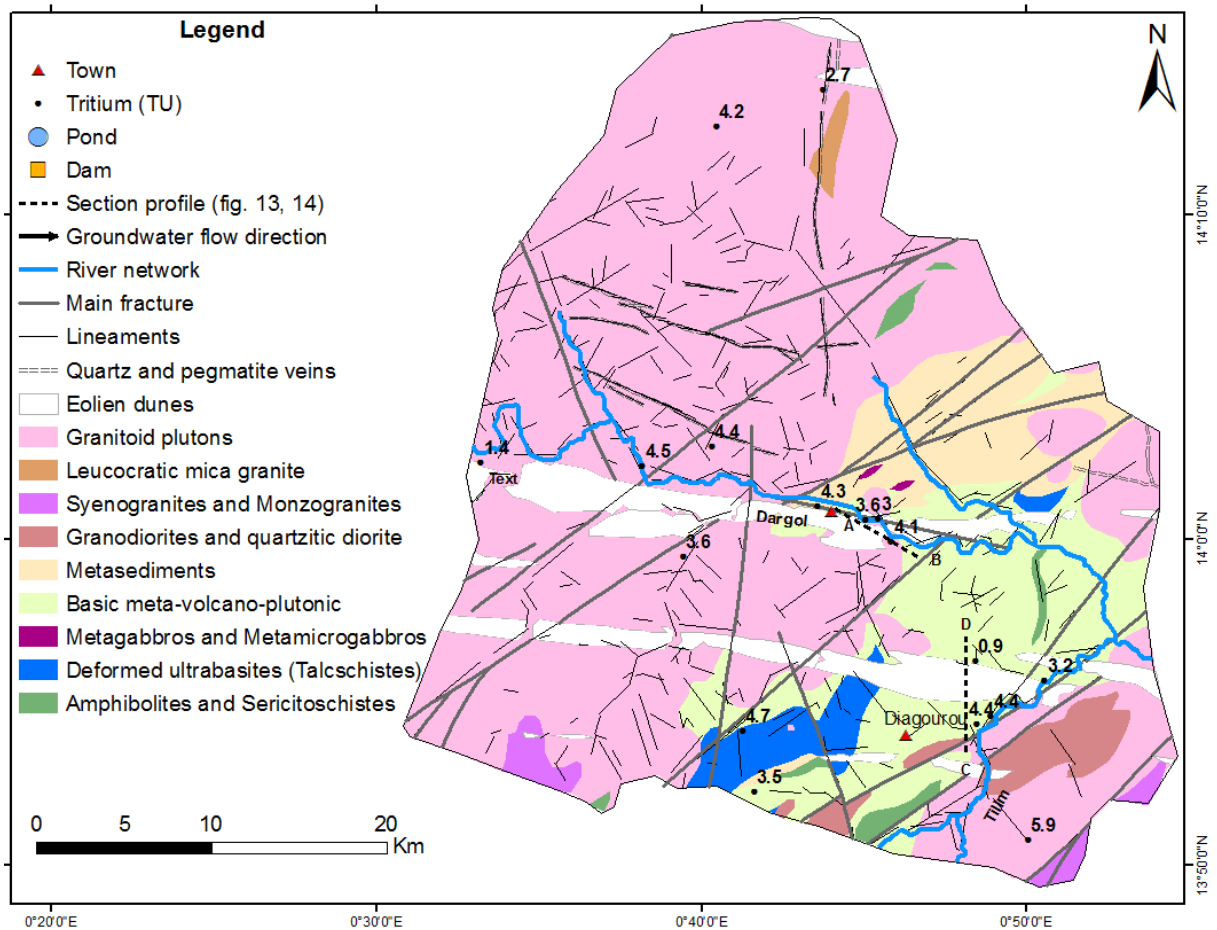


Fig. 3 Map of the main groundwater flow directions (Nov., 2009) in the deep aquifer part. Spatial distribution of the tritium content in groundwater.

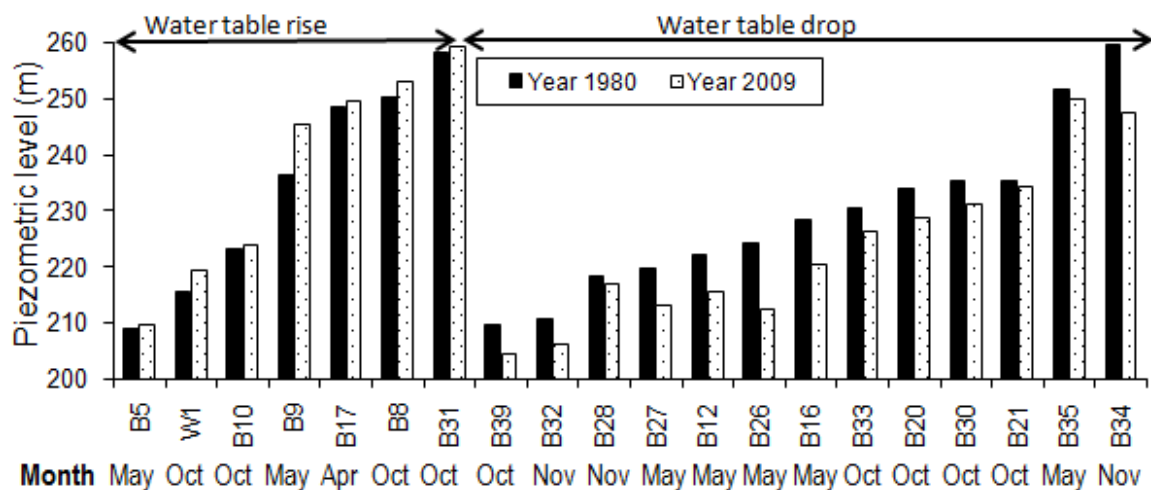


Fig. 4 Changes in groundwater levels between 1980 and 2009.

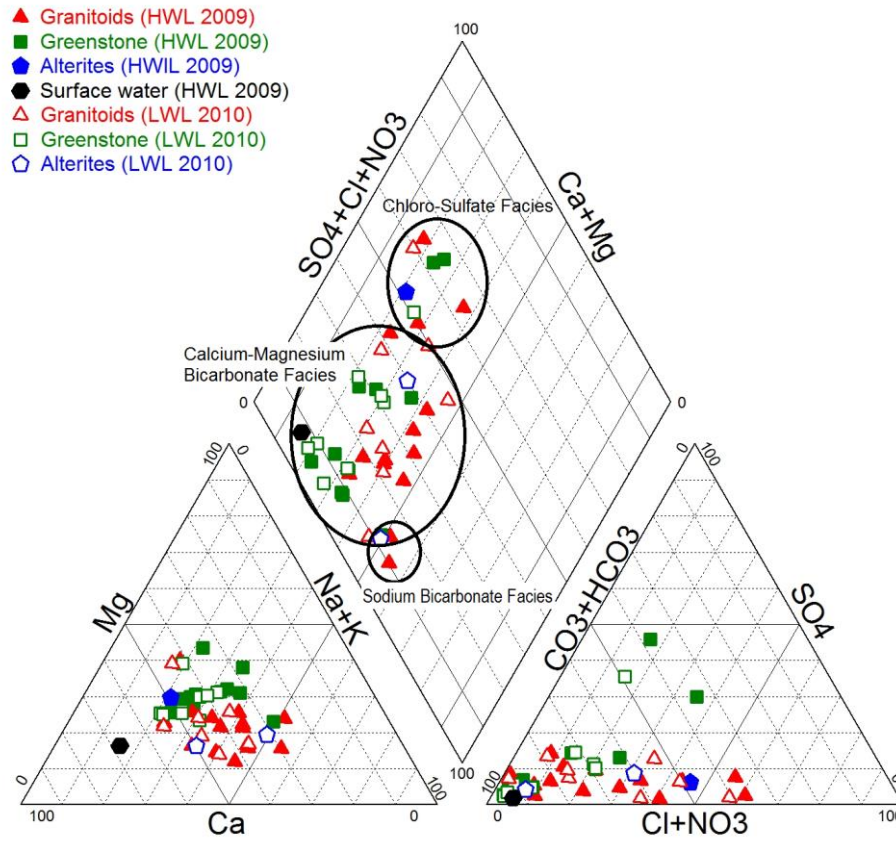


Fig. 5 Chemical facies (Piper diagram) of the sampled waters (HWL : High water levels; LWL : Low water levels)

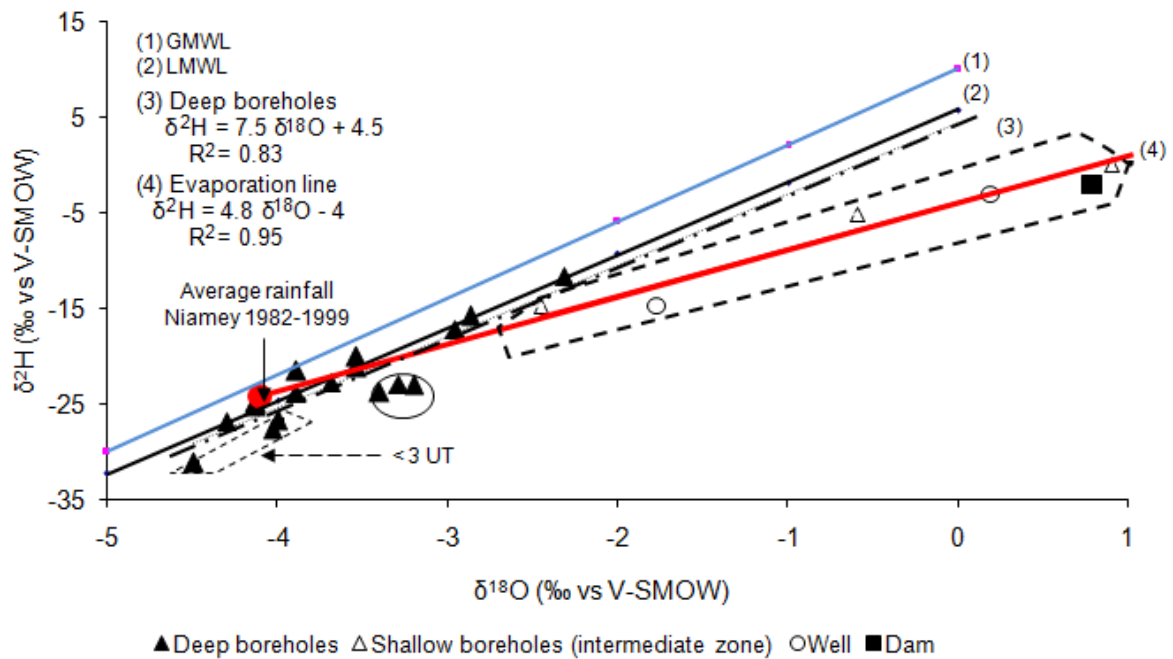


Fig. 6 Graph of $\delta^2\text{H}$ as a function of $\delta^{18}\text{O}$ for groundwater and surface water samples

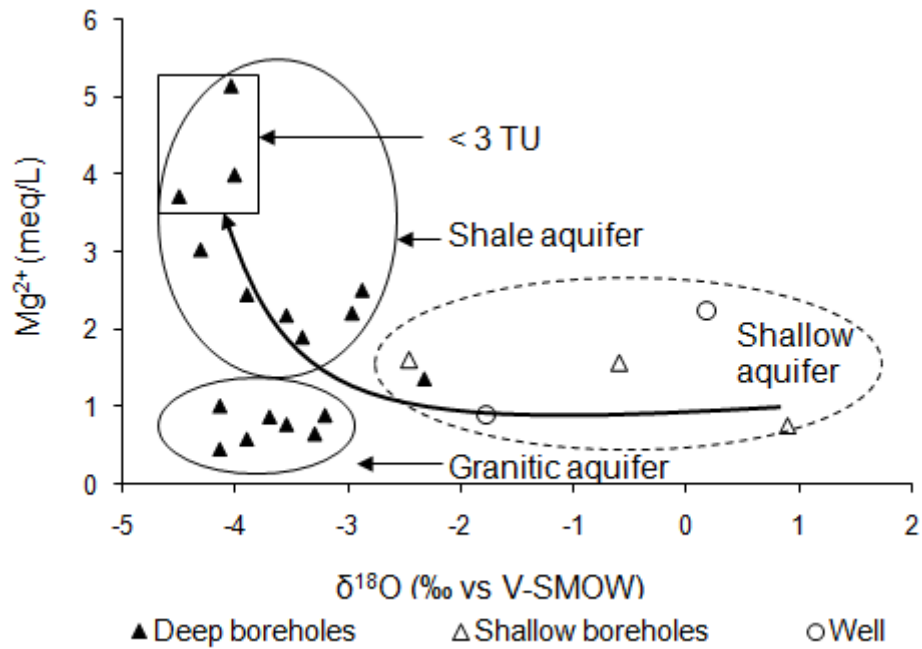


Fig. 7 Graph of magnesium (Mg^{2+}) as a function of oxygen-18 ($\delta^{18}\text{O}$) in groundwater. This relationship makes it possible to distinguish deep and confined schist aquifers, from granitic aquifers overlaid by sandy clay weathering products more permeable than those found above the schist formations.

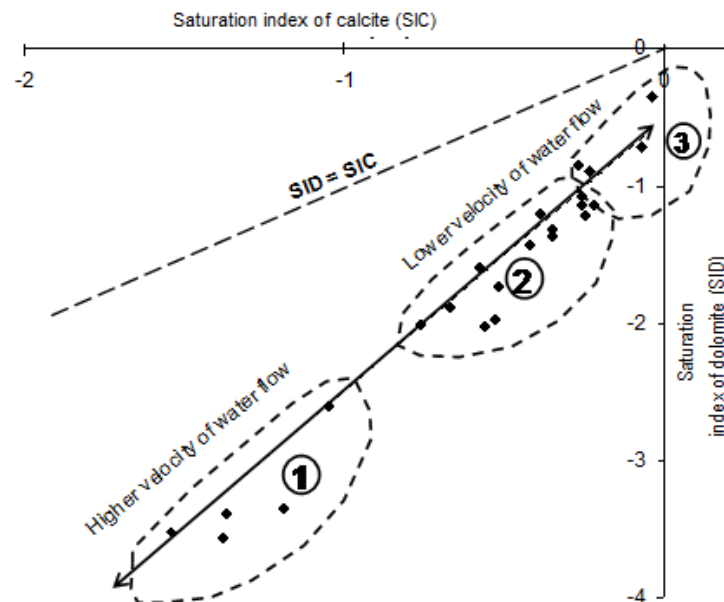


Fig. 8 Bivariate plot showing the relationship between the saturation index of calcite (SIC) and dolomite (SID) for the groundwater samples.

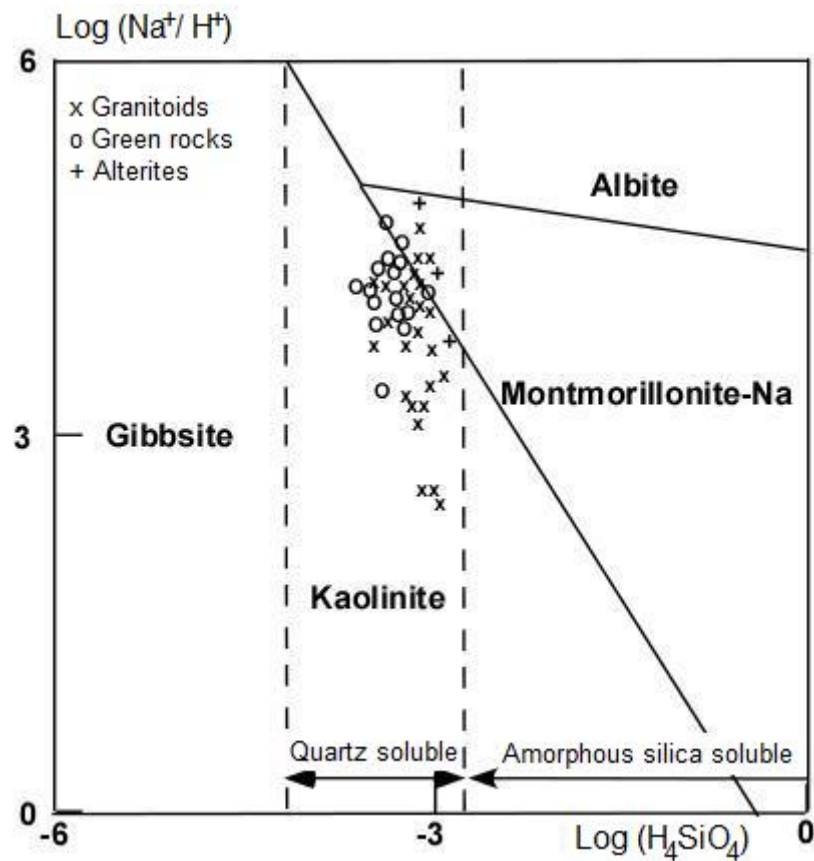


Fig. 9 Equilibrium diagram of albite-montmorillonite-kaolinite-gibbsite (at 25°C) for groundwaters in granitoid, green rocks and alterites.

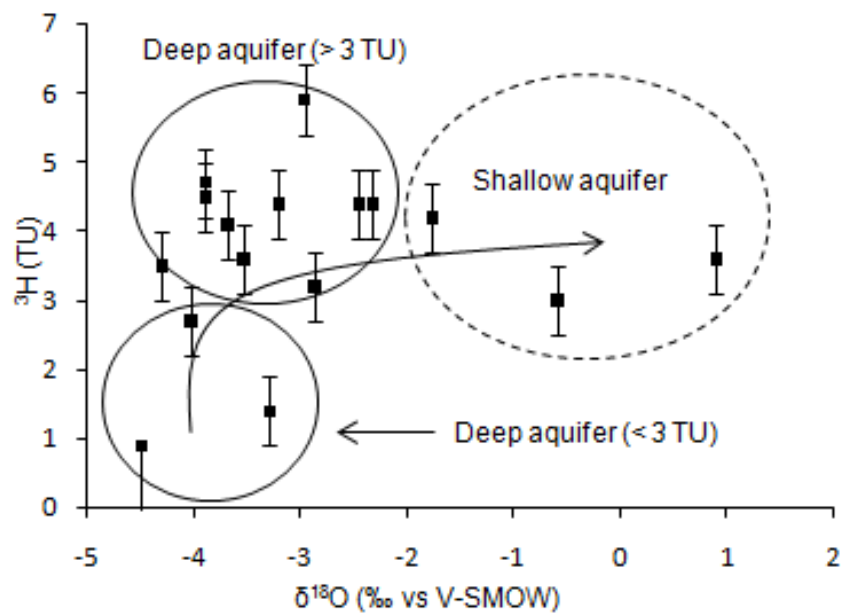


Fig.10 Graph of ^3H content as a function of $\delta^{18}\text{O}$ in groundwater.

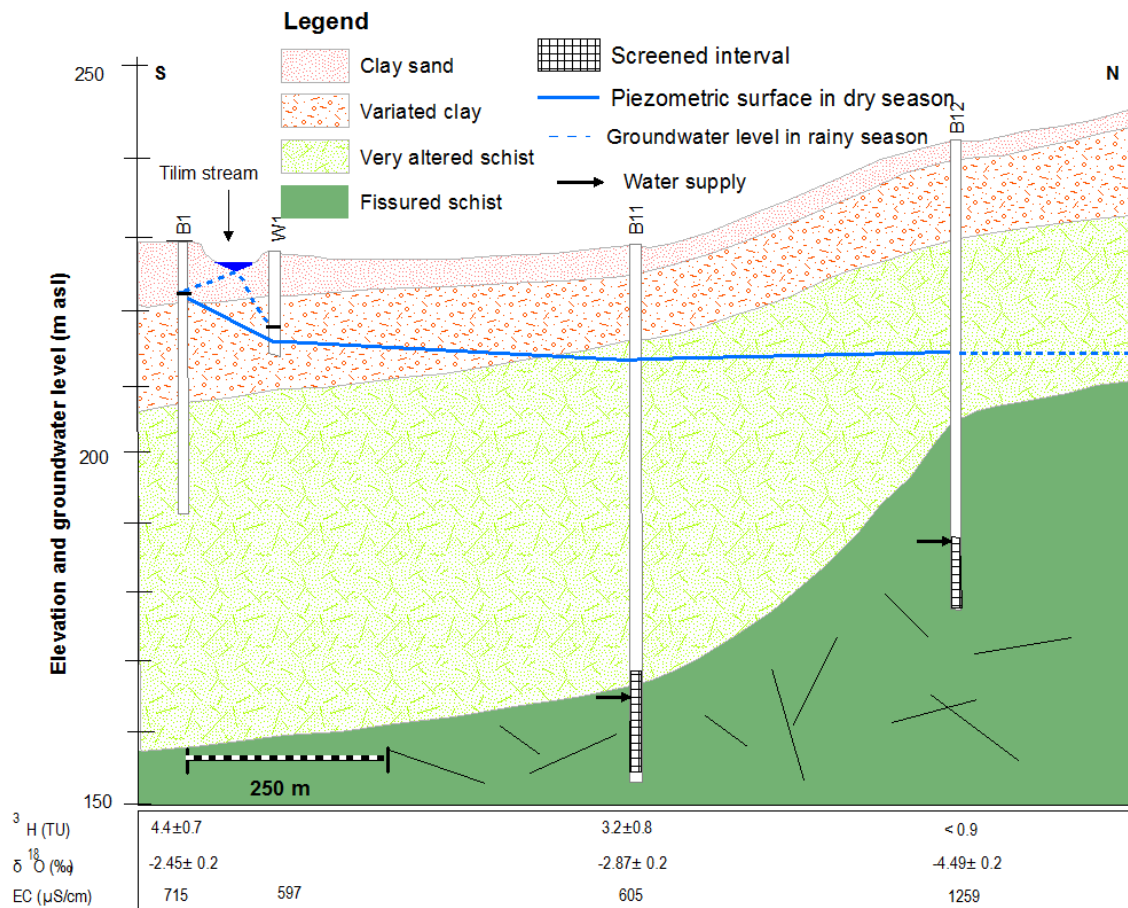


Fig 11 Geological cross-section (C-D axis in Fig.3) indicating the confinement of the deep aquifer under the alterite layer. Corresponding isotopic contents and electrical conductivity (EC) of groundwater measured in boreholes are reported.

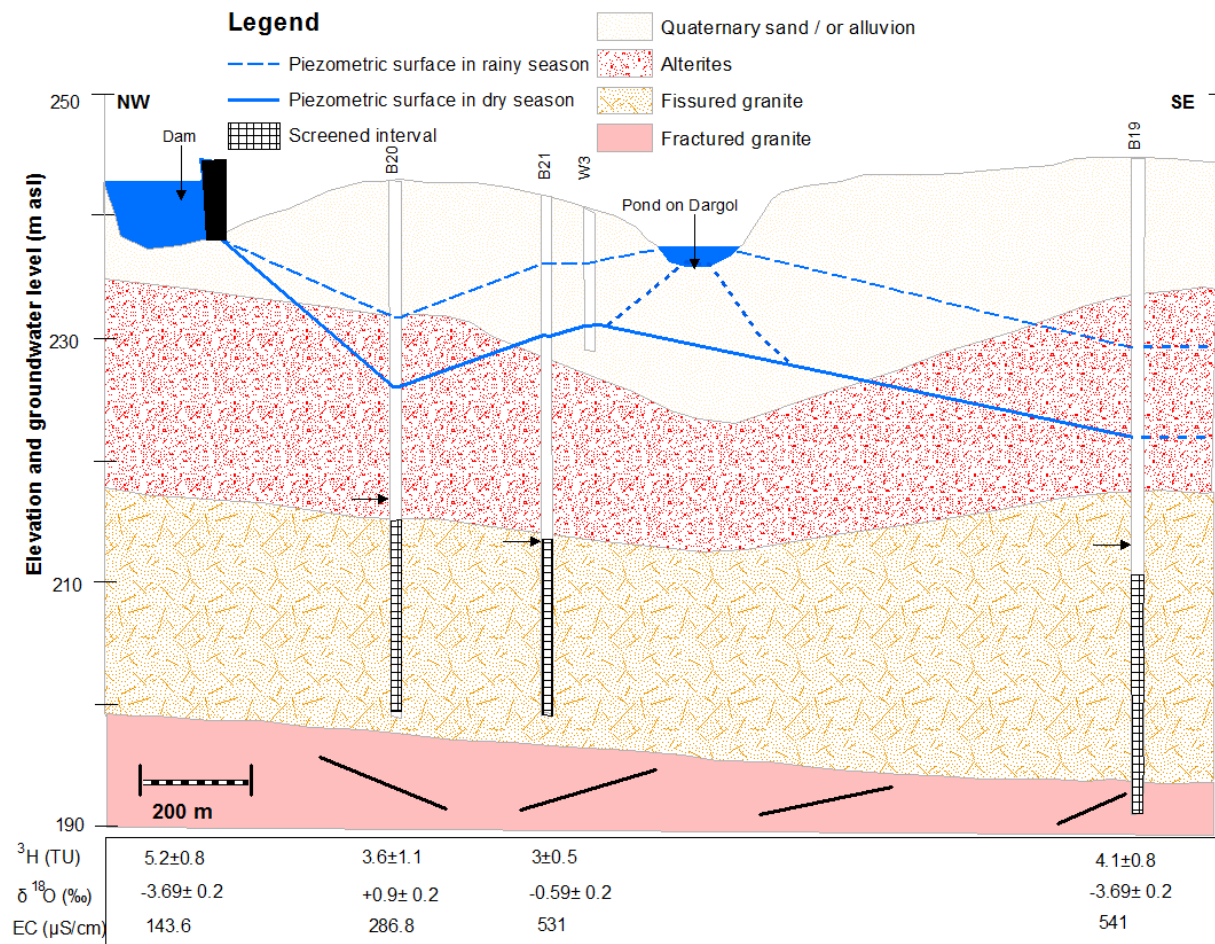


Fig. 12 Geological cross-section (AB axis in Fig.3) showing the direct hydraulic connection between both the shallow and deep aquifers in the granitic zone. Corresponding isotopic contents and EC of groundwater measured in boreholes are reported.